High-Resolution Phosphorus Nuclear Magnetic Resonance Spectroscopy of Transfer Ribonucleic Acids: Multiple Conformations in the Anticodon Loop†

David G. Gorenstein*,‡ and Evelyn M. Goldfield

ABSTRACT: The temperature dependence of the ^{31}P NMR spectra of yeast phenylalanine tRNA, *E. coli* tyrosine, glutamate (2), and formylmethionine tRNA is presented. The major difference between the ^{31}P NMR spectra of the different acceptor tRNAs is in the main cluster region between −0.5 and −1.3 ppm. This confirms an earlier assignment of the main cluster region to the undistorted phosphate diesters in the hairpin loops and helical stems. In addition the ^{31}P NMR spectra for all tRNAs reveal ~16 nonhelical diester signals spread over ~7 ppm besides the downfield terminal 3′-phosphate monoester. In the presence of 10 mM Mg^{2+} most scattered and main cluster signals do not shift between 22 and 66 °C, thus supporting our earlier hypothesis that ^{31}P chemical shifts are sensitive to phosphate ester torsional and bond angles. At >70 °C, all of the signals merge into a single random-coil conformation signal. A number of the scattered peaks are shifted (0.2–1.7 ppm) and broadened between 22 and 66 °C in the presence of Mg^{2+} and spermine as a result of a conformational transition in the anticodon loop. The ^{31}P NMR spectrum of the dimer formed between yeast $tRNA^{Phe}$ and *E. coli* $tRNA_2^{Glu}$ is reported. This dimer simulates codon–anticodon interaction since the anticodon triplets of the two tRNAs are complementary. Evidence is presented that the anticodon–anticodon interaction alters the anticodon conformation and partially disrupts the tertiary structure of the tRNA.

The ^{31}P NMR spectrum of yeast phenylalanine tRNA ($tRNA^{Phe}$) has been shown to contain considerable fine structure. High-resolution ^{31}P NMR[1] spectra by Gueron & Shulman (1975) and later by Salemink et al. (1979) and Gorenstein & Luxon (1979) revealed ~16 individual phosphate resonances spread over 7 ppm which were not observed in earlier ^{31}P tRNA spectra (Gueron, 1971; Weiner et al., 1974; Gorenstein & Kar, 1975).

At about the same time Gorenstein and co-workers had proposed that ^{31}P chemical shifts of phosphate esters are sensitive to changes in O–P–O bond angles and ester torsional angles (Gorenstein & Kar, 1975, 1977; Gorenstein, 1975, 1977, 1978, 1981; Gorenstein & Goldfield, 1982), and model system studies on single- and double-stranded nucleic acids (Gorenstein & Luxon, 1979; Gorenstein et al., 1976, 1981, 1982; Patel, 1976) suggested that a phosphate diester in a gauche,gauche (*g,g*) conformation should resonate several ppm upfield from a diester in a nongauche conformation. It has been suggested, therefore, that stereoelectronic (bond and torsional angle) differences are responsible for the 7 ppm spread in the ^{31}P signals of the tRNA. An initial attempt to simulate the ^{31}P spectra of $tRNA^{Phe}$ based upon the X-ray crystallographically determined phosphate ester torsional angles supported the suggestion that the shifts in the scattered peaks are due to both torsional and bond angle distortions associated with tertiary structure (Gorenstein & Luxon, 1979; Gorenstein et al., 1981).

The effect of Mg^{2+} and Mn^{2+} (Gorenstein et al., 1981) as well as nuclease treatment (Salemink et al., 1979) on the ^{31}P NMR spectrum of yeast $tRNA^{Phe}$ has been used to partially identify several of the scattered, single phosphate signals (Gorenstein et al., 1981; Gorenstein & Goldfield, 1982; Salemink et al., 1981). In a continuation of our studies on the solution conformation of tRNAs, we now present the ^{31}P NMR spectra of various other acceptor tRNAs.

Experimental Procedures

Yeast $tRNA^{Phe}$ and Escherichia coli. $tRNA^{Tyr}$, $tRNA_2^{Glu}$, and $tRNA^{fMet}$ were obtained from Boehringer Mannheim. Freshly boiled buffers and sterile glassware which had previously been leached for at least 1 h in 40% nitric acid were used.

Dialysis tubing was boiled for 1 h in 5% $NaHCO_3$ and 2% EDTA and then twice more in redistilled water for 1 h each to ensure removal of divalent metal ions. The tRNA (20 mg for $tRNA^{Phe}$ or 4 mg for the other tRNAs) was dissolved in 1–4 mL of glass redistilled water and dialyzed twice for at least 3 h at 4 °C against 1 L of buffer (0.1 M NaCl, 0.1 M cacodylate, and Mg^{2+} where indicated, pH 7.0) containing 10^{-2} M EDTA and then 16–48 h at 4 °C against 1 L of buffer containing 10^{-3} M EDTA (one or two changes). The sample was concentrated on an Amicon ultrafiltration cell by using a UM-2 filter to 0.4 or 1.6 mL. For the high-field NMR studies, tRNA solution plus 20% D_2O for field locking was placed in a Wilmad spherical microcell which in turn was inserted into a 12-mm or 20-mm o.d. NMR tube containing distilled water. In the low-field NMR studies the sample was placed in a 5-mm NMR tube.

High-field, Fourier transform ^{31}P NMR spectra were taken on Nicolet NTC-200 (80.9-MHz ^{31}P) or NTC-360 spectrometers (8.46 T; 145.7-MHz ^{31}P) with proton noise, two-level decoupling, 56° pulses, 4K data points, and 1.4-s recycle time. At low field, spectra were recorded on a Bruker WP-80 spectrometer at 32.4 MHz (^{31}P) with 70° pulses, 8K data points, and 2.05-s recycle times. The spectra were broad band ^{1}H decoupled. The temperature of the sample was controlled

† From the Department of Chemistry, University of Illinois, Chicago, Illinois 60680. *Received June 4, 1982.* Supported by research grants from the National Institutes of Health and the National Science Foundation. Purchase of the Bruker WP-80 spectrometer was assisted by a National Science Foundation departmental equipment grant. Support of the Purdue Biological NMR facility by the National Institutes of Health (RRO 1077) is acknowledged.

‡ Fellow of the Alfred P. Sloan Foundation.

[1] Abbreviations: NMR, nuclear magnetic resonance; ORD, optical rotatory dispersion; CD, circular dichroism; EDTA, (ethylenedinitrilo)-tetraacetic acid; tRNA, transfer ribonucleic acid.

0006-2960/82/0421-5839$01.25/0

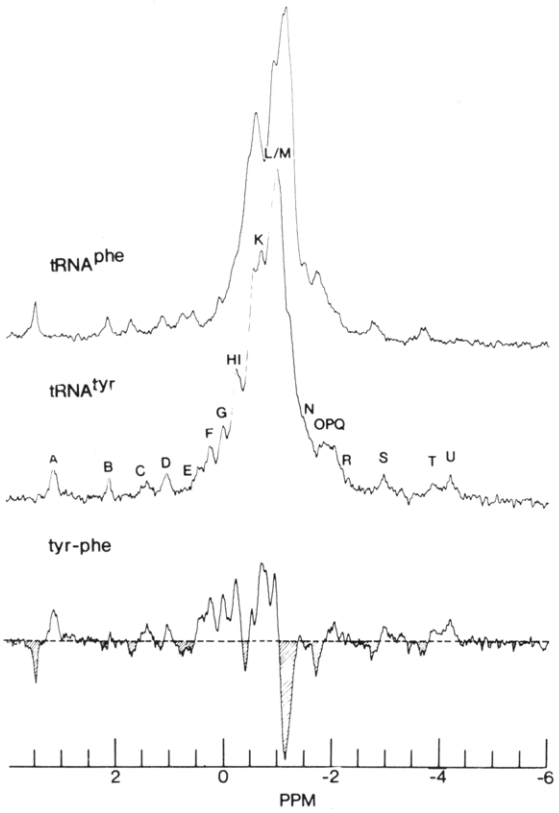

FIGURE 1: ^{31}P NMR spectra of yeast $tRNA^{Phe}$ (top) and *E. coli* $tRNA^{Tyr}$ (middle) and tyrosine – phenylalanine difference ^{31}P NMR spectrum (bottom) at 35 °C, pH 7, 10 mM $MgCl_2$, 100 mM NaCl, 10 mM cacodylate, 20% D_2O, and 1 mM EDTA, at 80.9 MHz (^{31}P) and 2-Hz line broadening applied to FID.

to within ±1 °C by Bruker or Nicolet temperature control units with nitrogen gas as a coolant. Decoupling at the superconducting fields produced about a 5–15 °C heating of the sample above the gas-stream measured temperatures, even when a gated two-level decoupling procedure was used [see Gorenstein & Luxon (1979)]. So that the solution heating could be corrected for by the decoupler, a ^{31}P "thermometer" as previously described (Gorenstein et al., 1981) was used.

Spermine·$tRNA^{Phe}$ samples were prepared by adding 5–20-μL aliquots of 0.08 M spermine buffer containing 10 mM Mg^{2+}, pH 7.0, to 0.6 mL of tRNA solution. Spermine hydrochloride was purchased from Sigma. The pH of the tRNA solution was checked after each addition of spermine buffer and was found to remain stable.

All chemical shifts were referenced to 15% phosphoric acid in D_2O (0.00 ppm) at room temperature (25 K). This sample is 0.453 ppm upfield from 85% H_3PO_4 with external D_2O lock. Positive chemical shifts are downfield from phosphoric acid.

tRNA spectral changes were reversible except that prolonged heating of some samples at $T > 60$ °C produced <1% nicks in the phosphodiester backbone. This was shown by the appearance of 2′,3′-cyclic nucleotide ^{31}P signals (Gueron & Shulman, 1975; Gorenstein & Kar, 1975) at ~20 ppm and additional phosphate monoester signals (at 3–4 ppm). All tRNA samples originally had no observable nicks in the backbone.

Results

^{31}P NMR Spectra of Different Acceptor tRNAs in 10 mM Mg^{2+}. A comparison of the ^{31}P NMR spectrum of yeast $tRNA^{Phe}$ and *E. coli* $tRNA_2^{Glu}$, $tRNA^{Tyr}$, and $tRNA^{fMet}$, in 10 mM Mg^{2+} buffer, ~30 °C, is shown in Figures 1 and 2. As Gueron & Shulman (1975), Salemink et al. (1979), and

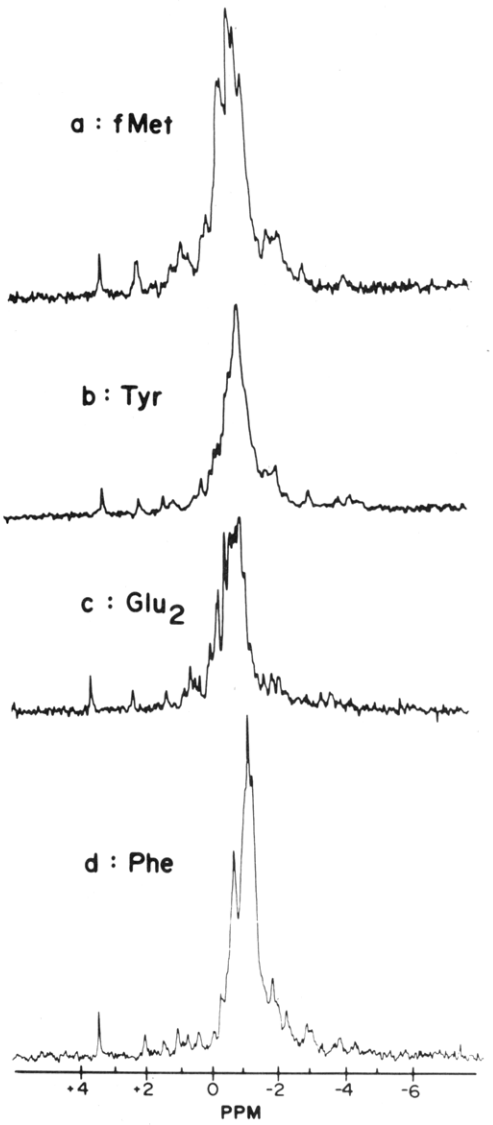

FIGURE 2: Comparison of ^{31}P NMR spectra of *E. coli* $tRNA^{fMet}$ (A), $tRNA^{Tyr}$ (B), $tRNA_2^{Glu}$ (C), and yeast $tRNA^{Phe}$ (D) at pH 7, 20% D_2O, 10 mM $MgCl_2$, 0.1 M NaCl, 10 mM cacodylate, and 1 mM EDTA, 31 °C (except $tRNA_2^{Glu}$ at 35 °C), at 32.4 MHz with 0.5 Hz spectral line broadening.

Gorenstein & Luxon (1979) have earlier shown for yeast $tRNA^{Phe}$, the other tRNAs also show a number of similar spectral features. Thus between +3.1 and +3.4 ppm is the 3′-terminal phosphate which integrates for a single phosphate residue and is the only signal which is pH sensitive (being a monoester with $pK \sim 6$). Between 0 and −1.5 ppm is a main cluster of signals representing the undistorted phosphate diesters in the double-helical stems and hairpin loops (see Discussion). The main cluster peaks L/M for the helical stems integrate for 35–37 phosphates in all the tRNAs. Upfield and downfield of the main cluster, spread over 6–7 ppm, are ~16 scattered signals, of which a number are well resolved at 30 °C. As shown in Figures 3 and 4, other scattered signals become better resolved at different temperatures. Individually resolved signals (such as B, C, D, and T) integrate in all tRNAs for ~1 phosphate.

The temperature dependence of the ^{31}P chemical shifts of the labeled signals in Figures 2–4 is shown in Figures 5–7. Between 20 and 60 °C most of the scattered and main cluster signals shift very little with temperature. As shown earlier (Gueron & Shulman, 1975; Salemink et al., 1979; Gorenstein & Luxon, 1979; references in Gorenstein & Goldfield, 1982)

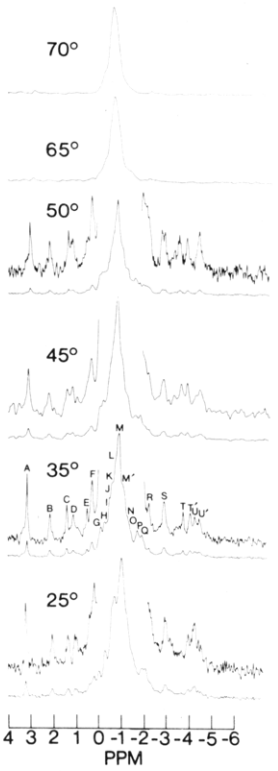

FIGURE 3: ^{31}P NMR spectra of *E. coli* tyrosine tRNA (2 mg/mL) in 0.1 M NaCl, 10 mM cacodylate, 10 mM $MgCl_2$, 1 mM EDTA, and 20% D_2O, pH 7, at indicated temperatures (°C). Expanded scale for the scattered peaks is shown over the normal spectrum. Number of acquisitions 4000–16 000 FIDs, 80.9 MHz, and 0.5 Hz line broadening.

this temperature insensitivity to most features in the tRNA ^{31}P spectra in 10 mM Mg^{2+} suggests that the tRNAs (and the backbone phosphates) largely retain their native conformation throughout this temperature range. Eventually at $T > T_m \sim$ 60–75 °C, all of the diester peaks merge into a single signal, with the tRNA melting into a random-coil conformation. The melting of the secondary and tertiary structure around 60–75 °C is confirmed in the UV melting curve of $tRNA^{Tyr}$ (see Figure 6).

Although the main cluster signals and most of the scattered peaks show only small shifts with temperature, several important exceptions are notable (see plots of Figures 5–7). For $tRNA^{Phe}$ (Figures 1 and 5) peak C shifts 0.55 ppm upfield from 22 to 50 °C while peak E shifts 0.4 ppm downfield. The two peaks and peak D (which shifts little) merge at 50 °C, and between 40 and 46 °C, the integrated intensity for the peaks decreases by 0.75 phosphate. At a higher temperature a new broad upfield peak (integrating for ~1 phosphate) shifts upfield away from the merged signals. Although it is not possible to definitely establish which of the three peaks disappears and which shifts further upfield, assuming the shift trends are continuous over the entire temperature range, it appears that peak C shifts ca. 1 ppm upfield and broadens while E shifts 0.6 ppm downfield with increasing temperature. Peak D shifts very little over this temperature range and does not broaden. Peaks F, P, T, and U are the only other peaks which display a large shift with temperature, shifting 0.3–1.7 ppm.

Assignment of the signals in the other tRNAs is based upon chemical shift comparisons to $tRNA^{Phe}$ ^{31}P spectra. The largest main cluster signals are assigned L and M and the downfield main cluster signals J/K. The temperature sensitivity and the relative chemical shifts to the the scattered

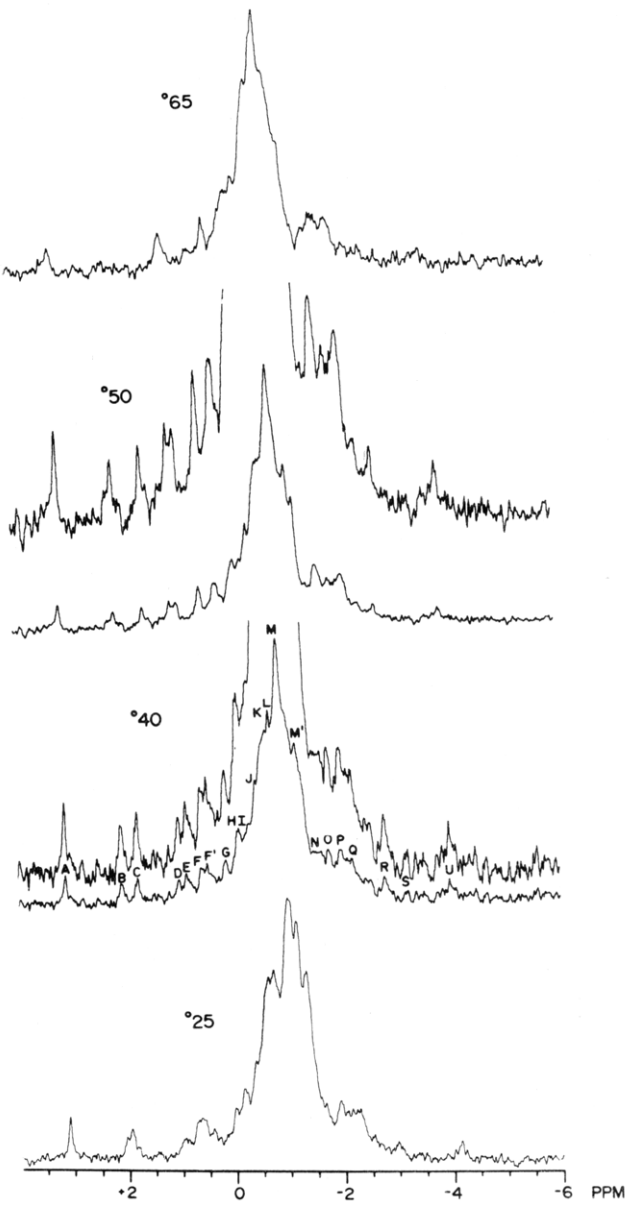

FIGURE 4: ^{31}P NMR spectra of *E. coli* formylmethionine tRNA (8 mg/mL) under similar conditions as in Figure 3, at 2 Hz line broadening and 10 000 FIDs.

signals were also used in making these assignments.

The temperature dependence of the chemical shifts for $tRNA^{Tyr}$ (Figures 3 and 6) differs somewhat from $tRNA^{Phe}$. Peak C shows almost no temperature dependence to its chemical shift between 20 and 60 °C (melting temperature is about 65 °C). Peak D shifts slightly upfield at higher temperatures, and peaks E and F both shift upfield with increasing temperature (as opposed to F shifting downfield in $tRNA^{Phe}$). The E and F resonances also appear further upfield than in the $tRNA^{Phe}$ spectra; peak E is at 0.25 ppm at 25 °C, and peak F is at ~0 ppm. There are three far upfield peaks T, U, and U′ which are all temperature dependent.

The $tRNA^{fMet}$ is the most stable of the tRNAs because it has more G-C base pairs than the other tRNAs, and its melting temperature at high Mg^{2+} is 75 °C. Therefore, at 70 °C, considerable tertiary structure remains, although the peaks have broadened substantially. The temperature dependence of the chemical shifts resembles that of $tRNA^{Phe}$ (Figures 4 and 7). However, peak C is located further upfield at ~2.0 ppm at 20 °C and merges with peak D at 65 °C, never moving as far upfield as it does in $tRNA^{Phe}$ (at least as a distin-

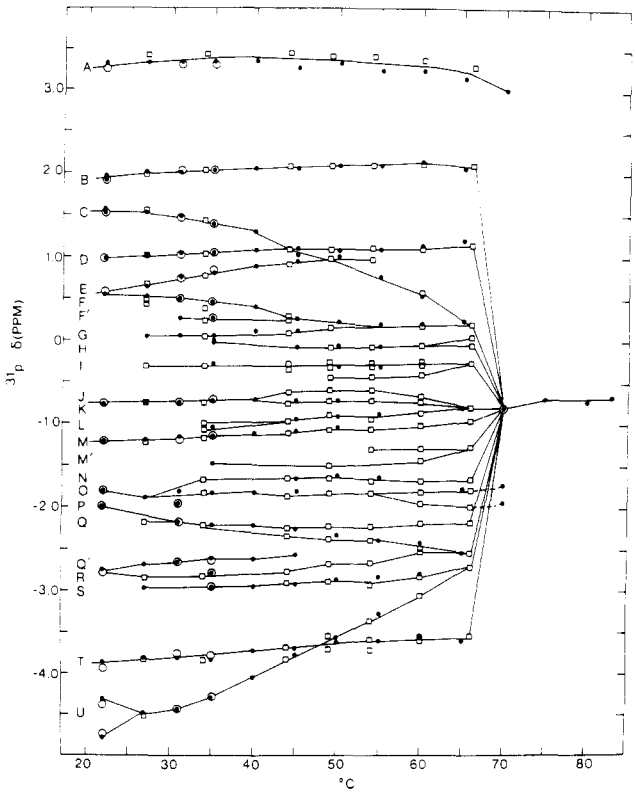

FIGURE 5: Temperature dependence of the chemical shifts, δ, in the peaks identified in Figure 1 for $tRNA^{Phe}$: (□) 145.8 MHz, (●) 32.4 MHz, and (○) repeat spectra at 32.4 MHz.

guishable peak). The behavior of peaks E, F, and F′ very much resembles that of $tRNA^{Phe}$. Peak U at −4.3 ppm at 20 °C moves downfield to −3.7 at 60 °C after which it disappears. There is no resonance corresponding to peak T of $tRNA^{Phe}$, but there are two temperature-dependent resonances (S and S′) which began appearing as one peak at 25 °C at −3.0 ppm and move downfield to −2.3 (S) and −2.55 ppm (S′) at 60 °C after which they also disappear. There is an anomalous upfield shift of these peaks between 30 and 35 °C (see Figure 7).

At no temperature does $tRNA_2^{Glu}$ exhibit the temperature-dependent resonance corresponding to peak C in the $tRNA^{Phe}$ or $tRNA^{fMet}$ spectra. However, there is a temperature-dependent U peak which shifts from −3.0 to −3.4 ppm between 20 and 55 °C. At 20 °C this peak integrates for 2 phosphates, but by 55 °C it has merged with other upfield resonances to integrate for 6 phosphates. At 35 °C there are two such peaks, one at −3.5 and the other at −3.7 ppm. The E, F, and F′ resonances are upfield from those in $tRNA^{Phe}$ (between 0.65 and 0.33 ppm). $tRNA_2^{Glu}$ also exhibits more fine structure in the main cluster region: at 35 °C there are well-defined peaks at −0.136, −0.393, −0.574, −0.655, −0.846, −0.921, and −1.027 ppm.

$tRNA^{Phe}$ and $tRNA^{fMet}$ ^{31}P Spectra, No Magnesium. At lower temperature (T < 30 °C) the ^{31}P NMR spectra of $tRNA^{Phe}$ and $tRNA^{fMet}$ in the absence or in the presence of 10 mM Mg^{2+} are basically quite similar (see Figures 4 and 8). Apparently even without Mg^{2+} but in 0.2 M total Na^+ (0.1 M added NaCl) the native secondary and tertiary structure is similarly stabilized for both tRNAs at lower temperatures. However, a number of differences do exist even at 19 °C. When the $tRNA^{Phe}$ solution was titrated with added Mg^{2+} [see Figure 10 of Gorenstein & Goldfield (1982)], it was possible to identify (Gorenstein et al., 1981) which signals in the absence of Mg^{2+} correspond to the signals in the presence of Mg^{2+}. At 19 °C without Mg^{2+} peak C of $tRNA^{Phe}$

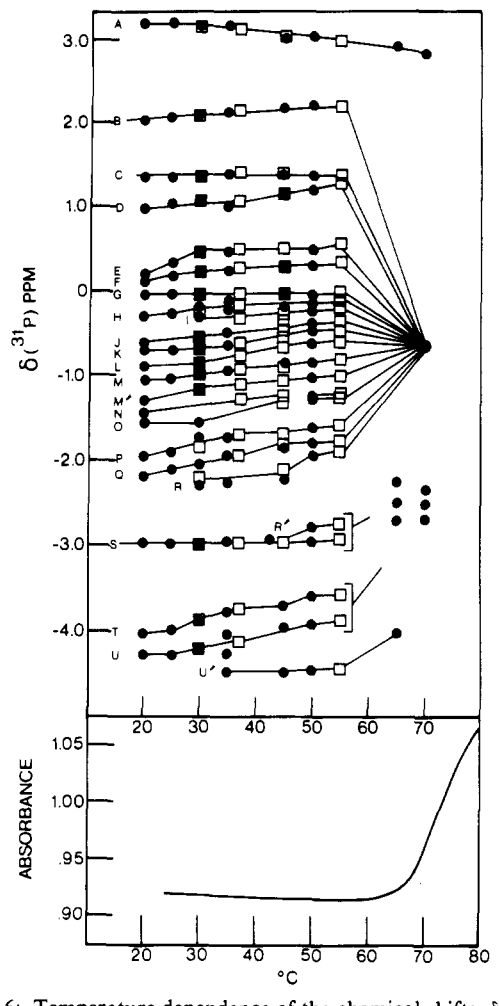

FIGURE 6: Temperature dependence of the chemical shifts, δ, in the peaks identified in Figure 3 for $tRNA^{Tyr}$. UV (260 nm) melting curve for sample, shown at bottom.

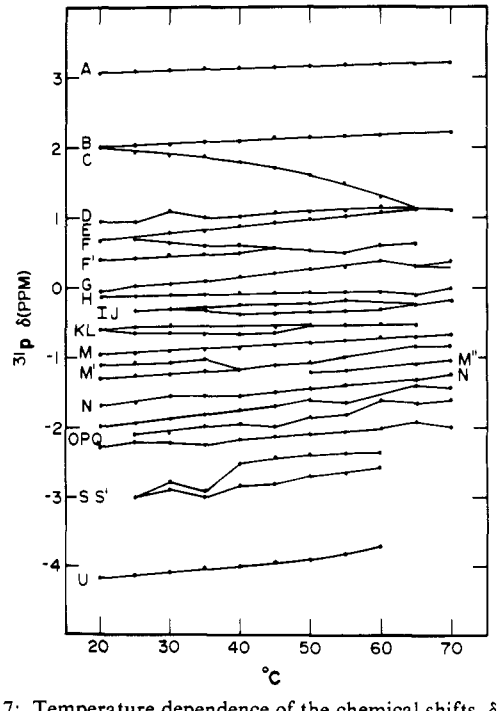

FIGURE 7: Temperature dependence of the chemical shifts, δ, in the peaks identified in Figure 4 for $tRNA^{fMet}$.

is shifted 1.0 ppm downfield relative to the high Mg^{2+} (10 mM dialyzed) sample while peak E is shifted 1.0 ppm upfield

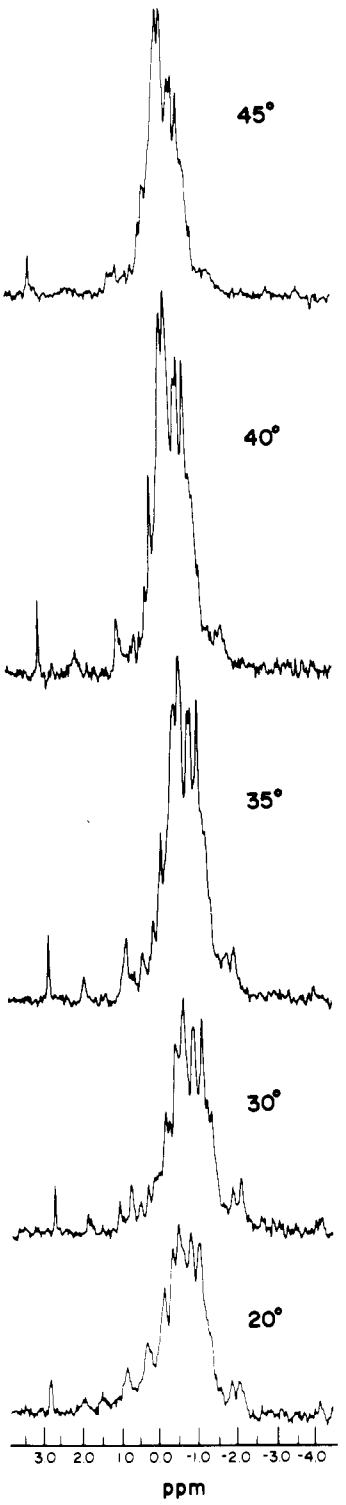

FIGURE 8: ^{31}P NMR spectra of $tRNA^{fMet}$ (8 mg/mL) in 100 mM NaCl, 10 mM cacodylate, 1 mM EDTA, and no Mg^{2+}, pH 7.0, at indicated temperatures (°C). At 32.4 MHz with 0.5 Hz spectral line broadening and 25 000–35 000 FIDs.

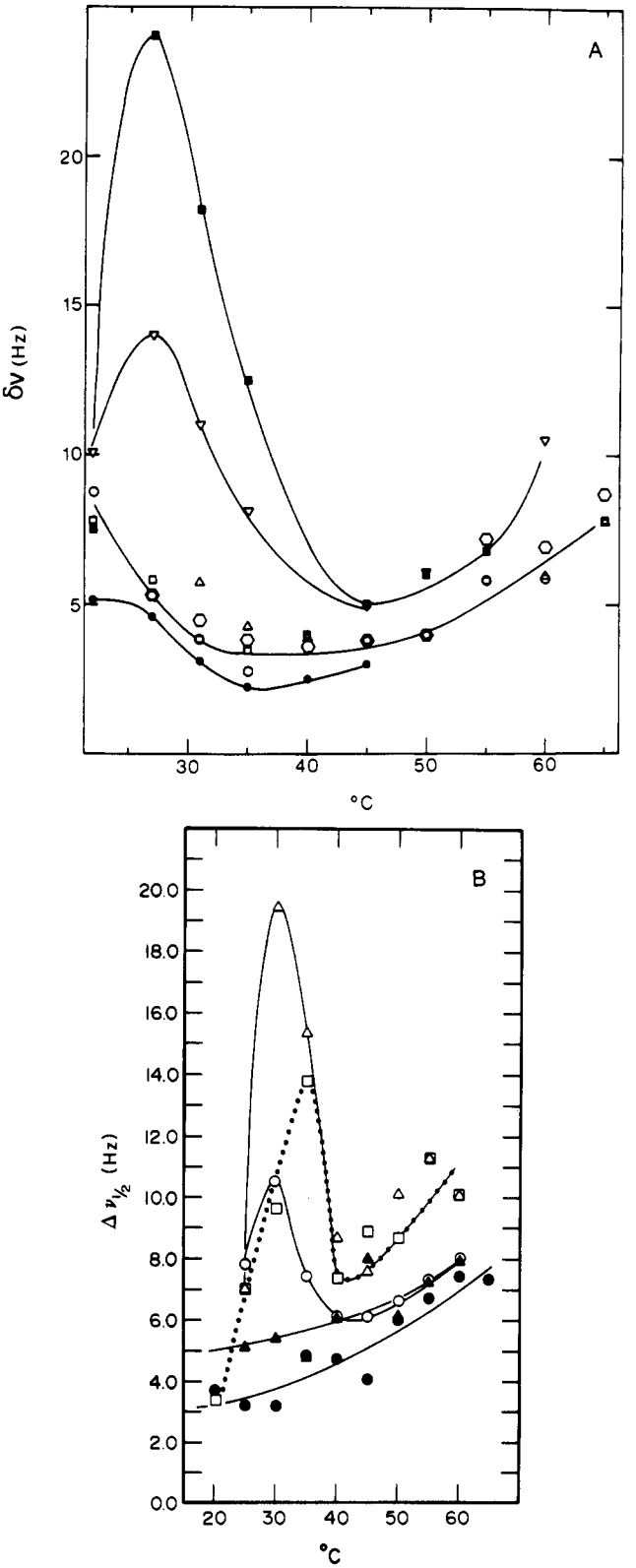

FIGURE 9: (A) Plot of the corrected line widths at half-height for scattered peaks at 32.4 MHz for $tRNA^{Phe}$ in 10 mM Mg^{2+} buffer for peaks A (●), B (○), C (○), D (□), E (△), T (▽), and U (■). (B) Plot of corrected line width for various scattered peaks for $tRNA^{fMet}$ vs. temperature; conditions described in Figure 4. Peak A (●), peak B (▲), peak C (○), peak S (△), and peak U (□).

relative to the high Mg^{2+} sample. Salemink et al. (1981) have found a similar reversal of peak C and E position at 30 °C as has Müller et al. (1980). [Our assignments are now in agreement with Salemink et al. (1979) and Müller et al. (1980)]. We have not assumed that the C and E signals in $tRNA^{fMet}$ are reversed in Mg^{2+} buffer (Figure 8) although no titration of the spectra with Mg^{2+} has been done.

In addition the integrated intensity for the scattered peaks (B–F; N–O) of $tRNA^{Phe}$ (and roughly the same for $tRNA^{fMet}$) is only ~3 in the absence of Mg^{2+} compared to 14 at 39 °C in 30 mM Mg^{2+}. At 19 °C, peaks B–E and N–U integrate for a total of 9 phosphates and 14 phosphates at 0 and 20 mM Mg^{2+}, respectively (Figure 8; Gorenstein et al., 1981). Corrected line widths at half-height ($\Delta\nu_{1/2}$) for some of the scattered signals of $tRNA^{Phe}$ and $tRNA^{fMet}$ at different tem-

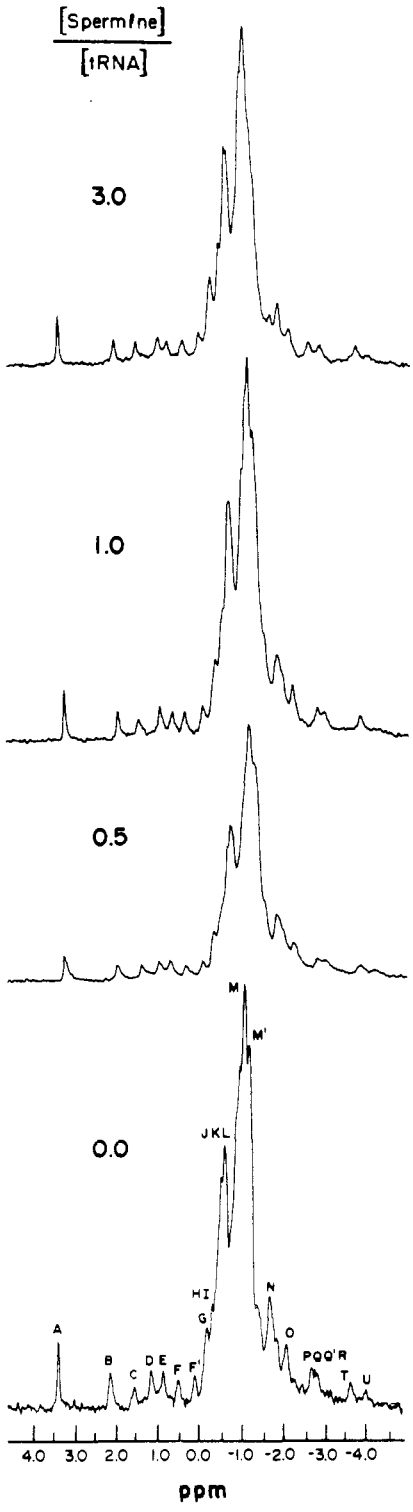

FIGURE 10: ^{31}P spectra of yeast $tRNA^{Phe}$ with added spermine at 31 °C, pH 7, 20% D_2O, 10 mM $MgCl_2$, 0.1 M NaCl, 10 mM cacodylate, and 1 mM EDTA at 32.4 MHz with 0.5 Hz spectral line broadening, 25 000–36 000 FIDs. Spermine:tRNA ratio: 0, 0.5, 1.0, and 3.0.

peratures are shown in Figure 9.

Effect of Spermine on $tRNA^{Phe}$ Spectra. The most striking effect of addition of spermine on the ^{31}P NMR spectrum of $tRNA^{Phe}$ is the broadening of the upfield peak U at −4.1 ppm. This line broadening varies with the spermine/tRNA ratio and reaches a maximum at the 1:1 ratio (Figures 10 and 11) at 31 °C. Other changes in the spectra are not as striking. Upon addition of spermine at 31 °C, the only other peaks which undergo significant line broadening are D, E, and F and perhaps P. Except for peak P, which does not broaden until

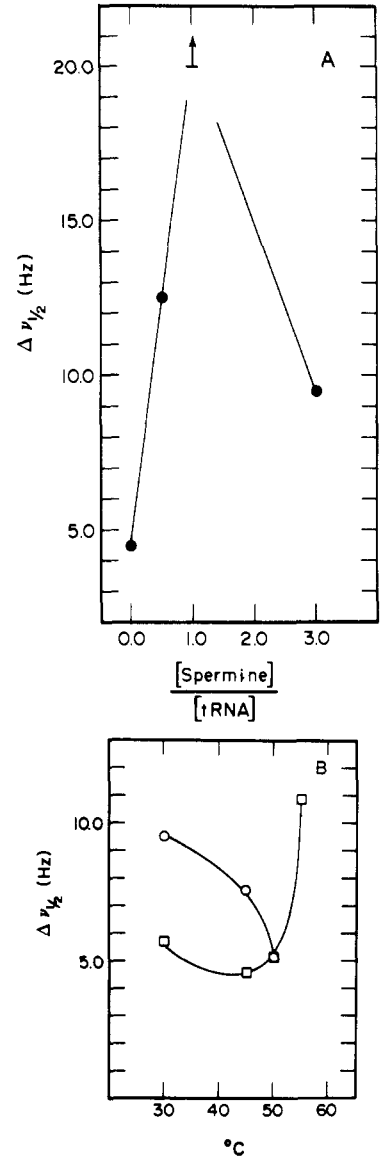

FIGURE 11: (A) Plot of corrected line width of peak U in $tRNA^{Phe}$ vs. (spermine:tRNA) ratio. Conditions: as in Figure 10. (B) Plot of corrected line widths of peak T (□) and peak U (○) vs. temperature, in yeast $tRNA^{Phe}$ with spermine:tRNA = 3.0.

the final addition of spermine, the other peaks broaden only about 1 Hz at the first addition of spermine and do not change significantly with further addition of spermine. The chemical shifts of the scattered peaks are not affected until the 3:1 ratio is reached. At this ratio, at 31 °C, peak D is shifted upfield by 0.1 ppm. Peaks N and O, which at 30 °C coalesce at −1.7 ppm in the absence of spermine, are split into separate peaks at −1.6 and −1.8 ppm. Also, the upfield peaks Q* and R are shifted downfield. Peak Q* is shifted from −2.73 to −2.54 ppm, and peak R is shifted from −2.84 to −2.79 ppm. These shifts of the upfield peaks reflect shifts which occur at higher temperatures in the absence of spermine. In the absence of spermine, peak O′ is at −2.54 at about 45 °C, and peaks N and O have split by ~1 Hz at around 35 °C. However, the temperature dependence of the chemical shifts is very similar to the dependence in the absence of spermine, and the two 55 °C spectra are almost identical.

^{31}P NMR of Yeast $tRNA^{Phe}$–E. coli $tRNA_2^{Glu}$ Complex. The anticodons of yeast $tRNA^{Phe}$ ($G^{2'OMe}AA$) and *E. coli* $tRNA_2^{Glu}$ (s^2UUC) are complementary, and the two form a strong complex through H-bonding interaction of the antico-

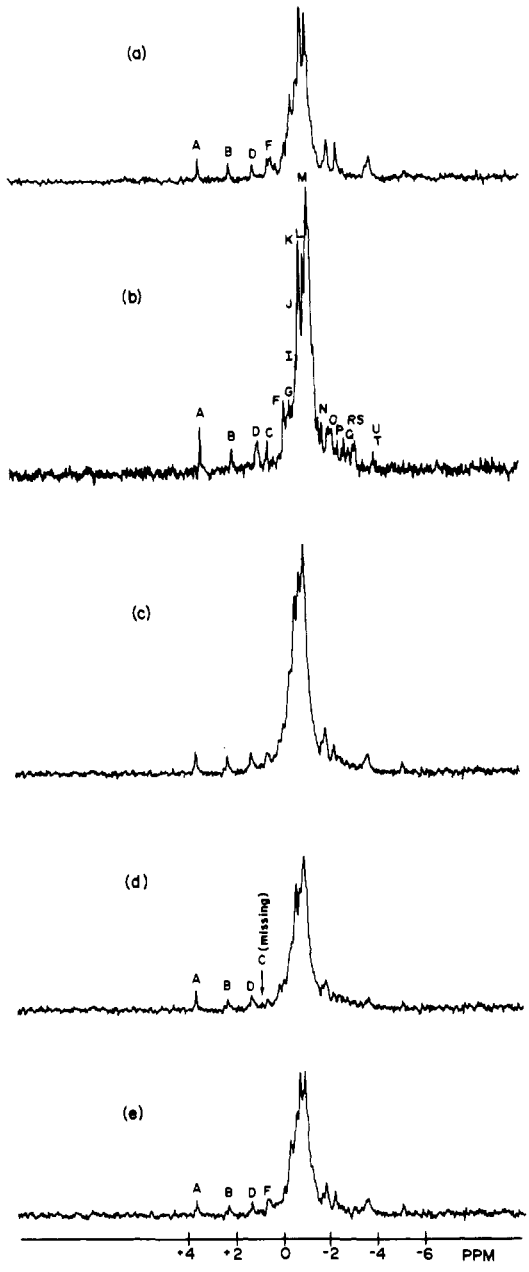

FIGURE 12: ^{31}P NMR spectra of *E. coli* $tRNA_2^{Glu}$ (a), yeast $tRNA^{Phe}$ (b), 1:1 complex (c), dimer minus $tRNA_2^{Glu}$ (d), and dimer minus $tRNA^{Phe}$ (e), 55 °C. 10 mM Mg^{2+} buffer, 32.4 MHz (25 000–35 000 scans).

dons (Eisinger, 1971; Grosjean et al., 1976). Comparison of the ^{31}P NMR spectra of the $tRNA^{Phe}$ and $tRNA_2^{Glu}$ alone and in a 1:1 complex at 55 °C is shown in Figure 12.

Discussion

Stereoelectronic Theory of ^{31}P Chemical Shifts: Application to tRNA Conformation. The observed coalescence of all of the diester signals of the tRNAs at ~70 °C in the presence of 10 mM Mg^{2+} is consistent with a stereoelectronic origin (bond/torsional angles; Gorenstein & Kar, 1975; Gorenstein, 1981) for these ^{31}P shift differences since at this temperature the native structure melts into a random-coil state. Except for some of the scattered signals (discussed below), the overall constancy of the ^{31}P spectra in the temperature range 22–66 °C is also consistent with the hypothesis that ^{31}P chemical shifts are sensitive to phosphate ester torsional angles and bond angles. The torsional angles are presumably constrained to fixed values in the native tRNA, and thus the ^{31}P signals shift little with temperature prior to disruption of this structure.

^{31}P NMR of Different Acceptor tRNAs. A study of the ^{31}P NMR spectra of tRNA can potentially provide important information on the solution backbone conformation and solution dynamics of these molecules. However, for this NMR probe to be most useful an assignment of some of the different scattered signals must be made. While present chemical shift theory is inadequate for this purpose, another proven method for spectral identification as shown in ^1H NMR studies (Reid & Hurd, 1979; Kearns, 1976) is to compare the NMR spectral features of different acceptor tRNAs. All tRNAs are now known to fit the cloverleaf secondary structure, and it is becoming increasingly clear that the tRNAs also have a tertiary structure quite similar to that found for yeast $tRNA^{Phe}$. Thus it is known from sequence studies that most of the conserved or semiconserved bases in different tRNAs are involved in tertiary structure hydrogen bonding (Kim et al., 1974). Recent low-resolution X-ray studies of $tRNA^{Gly}$ (Wright et al., 1979), $tRNA^{fMet}$ (Schevitz et al., 1979; Woo et al., 1980), and $tRNA^{Asp}$ (Moras et al., 1980) show that these molecules have structures similar to $tRNA^{Phe}$.

The yeast phenylalanine acceptor molecule is a class 1 (or D_4V_5) tRNA with four base pairs in the dihydrouridine stem, five bases in the variable loop, and a total of 76 nucleotides. *E. coli* $tRNA^{Tyr}$ is in class 2 (or D_3V_{13}) with a total of 85 bases, *E. coli* $tRNA_2^{Glu}$ is in class 1 (D_3V_4) with 76 nucleotides, and $tRNA^{fMet}$ is in class 1 (D_4V_5) with 77 nucleotides. In addition $tRNA^{fMet}$ differs from the other chain-elongating tRNAs in being the only tRNA that initiates protein synthesis. ^1H NMR studies (Reid & Hurd, 1979; Kearns, 1976) confirm that in most tRNAs there are about 20 (20 in $tRNA^{Phe}$ and 23 in $tRNA^{Tyr}$) base pairs stabilizing the secondary structure and 7 ± 1 tertiary structure base pairs. The $tRNA^{Tyr}$ largely differs from $tRNA^{Phe}$ and other class 1 tRNAs by the presence of the larger variable arm which presumably forms a helical hairpin loop that protrudes from the center of the molecule (Brennan & Sundaralingam, 1976). As shown by the ^{31}P difference spectra in Figure 1, most of the additional 9 phosphates in $tRNA^{Tyr}$ relative to the above class 1 tRNAs are found in the main-cluster spectral region (0 to −1.5 ppm) rather than in the scattered signals.

In tyrosine tRNA there are eight extra phosphates (relative to $tRNA^{Phe}$) in the variable arm, six of which can base pair and which are presumably in a double-helical $-g,-g$ conformation. The D loop in $tRNA^{Tyr}$, however, has one less base pair than $tRNA^{Phe}$ so only four more phosphates might be expected in the $-g,-g$ conformation. The other five extra phosphates in the $tRNA^{Tyr}$ structure are in the hairpin loops of the D and variable arms. From the ^{31}P difference spectra in Figure 1 we find extra phosphates in signals J, K, and L (and less in M) in $tRNA^{Tyr}$ relative to $tRNA^{Phe}$.

It is especially significant that few differences are found in the ^{31}P shifts of the scattered signals of the different acceptor tRNAs. The good agreement between the shifts of these scattered signals associated with the tertiary structures in the different tRNAs therefore provides further support to the belief that the tertiary structures of all tRNAs (even classes 1 and 2) are quite similar.

Temperature and Mg^{2+} Dependence of $tRNA^{Phe}$ ^{31}P Spectra. Magnesium stabilizes the functional, native conformation of tRNAs through stabilization of the loops and sharp turns in the tertiary structure (Kim, 1979). This explains the higher melting temperature of tRNAs in the presence of Mg^{2+}. The signals in the 10 mM Mg^{2+} dialyzed sample that show the largest temperature sensitivity are C, E, F, P, T, and

U (Figure 5). The signals that show the largest magnesium sensitivity are in $tRNA^{Phe}$ A, C, E, F, P, and T [U is not observed; Figures 4 and 5 in Gorenstein et al. (1981)]. Gorenstein et al. (1981) have suggested that the Mg^{2+} dependence of the chemical shifts of the scattered diester signals A, C, E, F, P, and T [and possibly U; see Salemink et al. (1981)] is likely due to a conformational change of the tRNA involving the tightly bound Mg^{2+} ions. The X-ray studies on yeast $tRNA^{Phe}$ have located the four strong magnesium binding sites. Magnesium in two of the sites cross-links the D and TΨC loops, and these are likely responsible for the cooperative stabilization of the tertiary structure by magnesium. A third magnesium binds to the AC loop. The temperature dependence of peaks C, E, F, P, T, and U in the 10 mM Mg^{2+} dialyzed sample likely reflects partial disruption of the binding site at higher temperature for one or more of these four tightly bound, tertiary structure stabilizing, magnesium ions. This high temperature (or low magnesium) conformation must retain most of the tertiary structure since UV and ^1H NMR melting studies (Reid & Hurd, 1979) under these conditions show no change in 3 °C structure.

Temperature Dependence of $tRNA^{fMet}$ (No Mg^{2+}). The temperature dependence of the ^{31}P NMR spectra of $tRNA^{fMet}$ in the absence of Mg^{2+} (Figure 8) is basically similar to that of $tRNA^{Phe}$ (Gorenstein & Luxon, 1979). Recall also that the chemical shifts of most of the scattered peaks of $tRNA^{fMet}$ at 20 °C are the same as those of $tRNA^{Phe}$ in the presence of 10 mM Mg^{2+} with the exception of peak C. For $tRNA^{fMet}$ peak C has been shifted upfield to 1.3 ppm, which is its chemical shift at 60 °C in 10 mM Mg^{2+}. As in $tRNA^{Phe}$, it appears that the $tRNA^{fMet}$ low magnesium conformation is similar to the high temperature, 10 mM Mg^{2+} conformation. Like $tRNA^{Phe}$, the peak C chemical shift does not remain constant as the Mg^{2+} sample is heated but continues to shift upfield until either it merges with peaks D and E at 65 °C or else it is broadened beyond detection.

Previous studies (Johnston & Redfield, 1981; Crothers, 1979) have assigned a melting temperature of 45–47 °C to the tertiary unfolding of $tRNA^{fMet}$ in the absence of Mg^{2+}, which is consistent with our data. By 36 °C, most of the scattered peaks integrate for less than one phosphate each, and by 45 °C there is general broadening and loss of intensity of the scattered peaks.

Line-Width Changes and Conformational Transitions. Previous optical (Sprinzl et al., 1974) and ^1H NMR studies (Kan et al., 1977; Reid & Hurd, 1979; Bolton & Kearns, 1977) have established that $tRNA^{Phe}$ retains its tertiary and secondary structure up to 65–70 °C in the presence of 10 mM Mg^{2+}. The overall constancy of the ^{31}P spectra for all tRNAs in the temperature range 22–66 °C is consistent with this conclusion, although some conformational changes are detected by ^{31}P NMR in this range. As shown in Figures 5–7, some of the scattered peaks show moderate upfield or downfield shifts with temperature. In addition, line broadening effects (Figure 9) suggest that a second lower temperature transition may be monitored with ^{31}P spectral changes.

The simplest model to analyze these results is in terms of a low-temperature (<50 °C) and high-temperature (>60 °C) transition. We suggest that transition I at lower temperatures is associated with the interconversion of two different conformations, both of which retain the main features of the secondary and tertiary structures found in the X-ray structure. Loss of the scattered signals' intensity (transition II) at higher temperature represents the cooperative melting of the secondary and tertiary structures into a random coil (Gorenstein & Luxon, 1979). The ^{31}P spectral changes (chemical shifts and line widths) observed in the lower temperature transition I are consistent with rapid chemical exchange between two (or possibly more) different tertiary conformations.

For most of the tRNA species, peaks C, D, E, F, P, T, and U shift with temperature between 22 and 60 °C. The line widths for the resolvable peaks, especially T and U, are similarly temperature sensitive. For $tRNA^{Phe}$ at 32 MHz, the line width of peak T increases from 10 to 14 Hz, and that of peak U increases from 8 to 24 Hz between 22 and 27 °C. With further increase in temperature, both signals resharpen to line widths of 5 Hz by ~45 °C (at 32 MHz; Figure 9A). At 146 MHz the line width for T increases from 22 Hz at 27 °C to 42 Hz at 49 °C. At 146 MHz, U broadens from ~70 Hz at 27 °C to 100 Hz at higher temperatures. Peaks C and U in $tRNA^{fMet}$ undergo similar line-width changes with temperature (Figure 9B). Peak U in *E. coli* $tRNA^{Tyr}$ shows similar chemical exchange line-broadening effects. At low temperature (<45 °C) the signal is too broad to be observed and only appears as it sharpens at $T > 35$ °C presumably due to fast exchange removing any chemical exchange line broadening.

The line-broadening maximum with temperature for peaks T and U and the frequency dependence of the line broadening are strong evidence for chemical exchange effects in transition I.

Most significantly the peaks that are most temperature and magnesium sensitive for this early transition I conformational change are largely in the anticodon loop [particularly C, E, F, and U, assigned in Gorenstein et al. (1981); see also Salemink et al. (1979)]. *Transition* I therefore likely *represents a conformational change in the anticodon loop*, supporting earlier suggestions (Labuda & Porschke, 1980, 1982; Gassen, 1980; Urbanke & Maass, 1978). Although highly speculative, we present one possible interpretation for this conformational change in the following discussion.

Besides their temperature sensitivity, peak C and peak E or U are also sensitive to magnesium ion (and E to manganese ion as well) (Gorenstein et al., 1981). It is potentially significant that temperature and magnesium ion have roughly an equal *and opposite* effect on the ^{31}P chemical shifts of peaks C and E/U. Thus C shifts ca. 1 ppm upfield with increasing temperature (20–65 °C) or decreasing magnesium concentration (10 mM Mg^{2+} free to 0) while E shifts 0.6–1.0 ppm downfield under similar changes. We have previously assigned peak C to the phosphate of Y_{37} and E/U to the phosphate of U_{33} (Gorenstein et al., 1981). They are involved in the divalent metal ion binding site(s) which must contribute to the stabilization of the anticodon loop conformation [Labuda & Porschke's (1982) magnesium binding AC loop conformation]. The roughly 1.0 ppm changes in the chemical shifts of C and E/U in this AC loop transition are about the right magnitude for rotation about one of the diester bonds from a gauche to a trans conformation or the reverse (Gorenstein, 1981). Thus P_{37} of Y_{37} (peak C) is in a $-g,t$ conformation (Sussman et al., 1978) and is directly stabilized by coordination to Mg^{2+}. Disruption of this structure by increasing the temperature or decreasing the magnesium ion concentration could alter the conformation about this phosphate to the lower energy $-g,-g$ (Gorenstein & Kar, 1977). P_{33} of U_{33} (peak E/U) is in a $-g,-g$ conformation at high magnesium and low temperature (at least from the X-ray structures; Sussman et al., 1978). Loss of magnesium (either by increasing the temperature or decreasing the magnesium concentration) could allow P_{33} to assume a $-g,t$ conformation, stabilized by the hydrogen bond between the N_3H of U_{33} and P_{36} (Sussman et al., 1978; Quigley et al., 1975;

Jack et al., 1976). This hydrogen-bonded arrangement is observed in the X-ray structures and helps provide for the "U-turn" in the phosphate ester backbone of the AC loop.

This magnesium-sensitive AC loop conformational change could be biochemically significant. It is well-known that magnesium ion is essential for the proper function of the tRNA in the translation process (Gassen, 1980). Urbanke & Maass (1978) have also noted a similar low-temperature conformational change in the AC loop as monitored by Y_{37} fluorescence changes. Proton NMR chemical shift changes of Y base methyl signals are also consistent with a change in the stacking arrangement of the anticodon triplet ($mG_{34}A_{35}A_{36}$) and Y_{37} (Davanloo et al., 1979). This AC loop conformational change could represent a shift from the AC triplet 3′-stacked conformation to a 5′-stacked conformation, as first suggested by Fuller & Hodgson (1967). Only two bases would remain stacked on the 3′ side in the 5′-stacked conformation (the triplet and two other bases are stacked on the 5′ side). The reverse is true for the 3′-stacked conformation. Since the major conformational flexibility in the tRNA backbone is about the phosphate ester bond (Stout et al., 1978), it is reasonable that the two "pivot points" for this conformational change are two phosphates. They simply switch between $-g,-g$ and $-g,t$ conformations.

This analysis gains additional support from the recent X-ray structure of *E. coli* initiator $tRNA^{fMet}$ (Woo et al., 1980). Overall the yeast $tRNA^{Phe}$ and *E. coli* $tRNA^{fMet}$ structures are quite similar. A major difference, however, exists in the anticodon loop, where on the initiator tRNA, uracil-33 has an almost opposite orientation to that found in $tRNA^{Phe}$. In the latter, U_{33} folds into the AC loop, with N_3 of U_{33} forming a hydrogen bond with phosphate 36. In $tRNA^{fMet}$ U_{33} is rotated into the solvent region, and a hydrogen bond is perhaps made between the 2′-OH of ribose 33 and phosphate 36. The oppositely rotated U_{33} in $tRNA^{fMet}$ could represent the high-temperature, low magnesium anticodon loop conformation. No divalent metal ion sites have yet been described in the X-ray structure for $tRNA^{fMet}$, and it would be significant if one was either not found or located in a different position than in $tRNA^{Phe}$.

The conformational change in the anticodon loop has been suggested to be an important event in protein biosynthesis (Woese, 1970; Lake, 1977). Thus in the Lake (1977) model the anticodon conformation switches from a 5′ stack to a 3′ stack after the correct recognition of the tRNA in the ribosome site. This would presumably allow the aminoacyl group to move toward the ribosome-bound peptidyl-tRNA.

Spermine·$tRNA^{Phe}$ ^{31}P Spectral Changes. A major effect of added spermine on the $tRNA^{Phe}$ ^{31}P NMR spectra is in the additional line broadening of peak U at 31 °C (Figure 11). Previous spectra on different $tRNA^{Phe}$ samples have shown variable line widths for peak U at ~30 °C. Salemink et al. (1979) had noted a sharpening of peak U upon phenol extraction of $tRNA^{Phe}$. Residual quantities of spermine in the dialyzed tRNA samples may be responsible for these effects. Cohen (1972) has shown that tRNAs bind ten molecules of spermine and that two or three spermine molecules are tightly bound [similarly reported by Schreier & Schimmel (1975)]. Takeda & Ohnishi (1975) have found that spermine is, in fact, more tightly bound than Mg^{2+}. Either dicationic magnesium or tetracationic spermine $[NH_3^+(CH_2)_3NH_2^+)$-$(CH_2)_4NH_2^+(CH_2)_3NH_3^+]$ can convert tRNA from an inactive conformation to an active conformation (Cohen, 1972), at least as monitored by the ability of the tRNA to be aminoacylated (Tabor & Tabor, 1976; Kayne & Cohn, 1972). Two of these bound spermine molecules have been resolved in the X-ray structure of $tRNA^{Phe}$ (Quigley et al., 1978). One spermine binds in the deep groove of the anticodon double-helix stem, apparently hydrogen bonded to four different phosphate residues. The positively charged spermine appears to draw the phosphates on opposite sides of the groove 3 Å closer together than might be expected in its absence. The second spermine binds at the beginning of the D stem near the top of the AC stem; it wraps around phosphate 10 and neutralizes the charge interaction between phosphates 9, 10, and 11 of one chain and phosphates 47, 46, and 45 of the other. Together with the two bound magnesium ions in the D and AC arms, the spermine immobilizes the AC end of the tRNA.

The line-width and chemical shift changes of the scattered signals that we have observed in the presence of spermine are consistent with the X-ray results. As discussed above the low-temperature conformational transition (I) is associated with a change in the anticodon loop conformation. Peak U has been assigned to the anticodon loop (Salemink et al., 1979; Gorenstein et al., 1981), and at the 3:1 spermine:tRNA ratio peak U narrows at higher temperatures (Figure 11). If one compares the line-width behavior of peak U with that of peak T which is typical of the other peaks, one sees that peak T remains relatively constant until 55 °C, where it broadens due to the slow chemical exchange between native structure and random coil. Although the line width of peak U cannot be measured at 55 °C (since it has merged with peak R), it is reasonable to suppose it further broadens at higher temperature. The narrowing of peak U as the temperature is increased is what one would expect if the broadening of this peak is due to chemical exchange, between the two conformations of the anticodon loop.

$tRNA_2^{Glu}$·$tRNA^{Phe}$ Dimer. The $tRNA^{Phe}$·$tRNA_2^{Glu}$ dimer ^{31}P resonances were too broad to analyze at 30 and 35 °C, so spectral comparisons with the monomers were made at 55 °C. The increased line width is attributed to the longer rotational correlation time of the larger dimer. By use of the thermodynamic constants of Eisinger & Gross (1975) for dimer formation, the equilibrium constant is calculated to be 6.8×10^4 at 55 °C. At our concentrations of 0.5 mM in each of $tRNA_2^{Glu}$ and $tRNA^{Phe}$, the ratio of dimer to each monomer should be greater than 5:1. The dimer also melts 5–10 °C higher (80 °C) than either monomer under comparable conditions.

The most striking features of the dimer spectra are (1) the complete absence of intensity of peak C, the temperature variable peak which is absent also in $tRNA_2^{Glu}$ and assigned to Y_{37} in $tRNA^{Phe}$, and (2) an apparent gain in intensity in the main cluster. This region accounts for 50–53 phosphates in each of $tRNA_2^{Glu}$ and $tRNA^{Phe}$ and at first inspection ~124 resonances in the dimer. However, the dimer main cluster is broader than in either $tRNA_2^{Glu}$ or $tRNA^{Phe}$ so that it covers up some of the upfield resonances between −1.0 and −1.4 ppm which are resolved in the individual tRNA monomer spectra and which integrate in total for six resonances. Therefore, the main cluster peaks actually account for ~118 phosphates, still larger than the expected 100–106. This increase in the main cluster peak area is largely due to an increase in peak I and in the dimer accounts for approximately ten more phosphates than expected. The other striking difference is the reduction in the intensity of the upfield scattered peaks, where it appears that at least ten phosphates have disappeared. Finally, a new far upfield peak which integrates for *0.5* phosphate has appeared in the dimer at −4.862 ppm. No peak has ever been observed so far downfield in any tRNA monomer

spectra at 55 °C, although this signal likely arises from the phosphate assigned to peak U.

These features of the dimer spectra argue strongly that there are at least three conformations for $tRNA^{Phe}$ at high Mg^{2+} (below T_m). The disappearance (or perhaps upfield shift) of peak C in the dimer strongly suggests that the AC loop has undergone a conformational change upon codon binding and that this conformation is different from either of the AC loop conformations described previously. The loss of upfield intensity indicates loss or modification of tertiary structure, since these peaks are associated with tertiary structure. This loss is similar to the spectral changes observed upon treatment with RNase T_1 which cleaves in the TΨC and D loops of tRNA disrupting the tertiary structure: the upfield resonances decrease from a total of 11 phosphates to 3 (Salemink et al., 1979). Also, the growth of the downfield portion of the main cluster which is where we find unstrained hairpin loop *g,g* phosphates indicates that the phosphates that were once in the tertiary folds of the tRNA are now in relatively free hairpin loops. Thus the tertiary structure has been *considerably* opened up. This conclusion is supported by equilibrium binding studies which have suggested that codon–anticodon recognition induces a partial unfolding of the tertiary structure, making part of the TΨC loop (TΨCG sequence) available for complementary base pairing to CGAA (Schwarz et al., 1974; Moller et al., 1978). Chemical modification (Wagner & Garrett, 1978) and fluorescence (Robertson et al., 1977) experiments have supported this conclusion, while proton NMR studies (Davanloo-Malherbe et al., 1978; Geerdes et al., 1978) have suggested that no (or very minor) changes occur upon codon–anticodon complexion. ^{31}P NMR appears to be a uniquely sensitive magnetic resonance probe for these subtle conformation changes in tRNA structure.

Acknowledgments

We acknowledge the contributions of Bruce Luxon and Rouhlwai Chen to these studies.

References

Bolton, P. H., & Kearns, D. R. (1977) *Biochemistry 16*, 5729.

Brennan, T., & Sundaralingam, M. (1976) *Nucleic Acids Res. 3*, 3525.

Cohen, S. S. (1972) *Adv. Enzyme Regul. 10*, 207–223.

Crothers, D. M. (1979) *Transfer RNA: Structure, Properties, and Recognition* (Schimmel, P. R., Soll, P., & Abelson, J. R., Eds.) pp 163–176, Cold Spring Harbor Laboratories, Cold Spring Harbor, NY.

Davanloo, P., Sprinz, M., & Cramer, F. (1979) *Biochemistry 18*, 3189–3199.

Davanloo-Malherbe, P., Sprinzl, M., & Cramer, F. (1978) *Jerusalem Symp. Quantum Chem. Biochem. 11*, 125.

Eisinger, J. (1971) *Biochem. Biophys. Res. Commun. 43*, 854–861.

Eisinger, J., & Gross, N. (1975) *Biochemistry 14*, 4031–4041.

Fuller, W., & Hodgson, A. (1967) *Nature (London) 215*, 817–821.

Gassen, H. G. (1980) *Prog. Nucleic Acid Res. Mol. Biol. 24*, 57–86.

Geerdes, H. A. M., Van Boom, J. H., & Hilbers, C. W. (1978) *FEBS Lett. 88*, 27–32.

Gorenstein, D. G. (1975) *J. Am. Chem. Soc. 97*, 898–900.

Gorenstein, D. G. (1977) *J. Am. Chem. Soc. 99*, 2254–2258.

Gorenstein, D. G. (1978) *Jerusalem Symp. Quantum Chem. Biochem. 11*, 1–15.

Gorenstein, D. G. (1981) *Annu. Rev. Biophys. Bioeng. 10*, 355–386.

Gorenstein, D. G., & Kar, D. (1975) *Biochem. Biophys. Res. Commun. 65*, 1073–1080.

Gorenstein, D. G., & Kar, D. (1977) *J. Am. Chem. Soc. 99*, 672–677.

Gorenstein, D. G., & Luxon, B. A. (1979) *Biochemistry 18*, 3796–3804.

Gorenstein, D. G., & Goldfield, E. M. (1982) *J. Mol. Cell. Biochem. 46*, 97.

Gorenstein, D. G., Findlay, J. B., Momii, R. K., Luxon, B. A., & Kar, D. (1976) *Biochemistry 15*, 3796–3803.

Gorenstein, D. G., Goldfield, E. M., Chen, R., Kovar, K., & Luxon, B. A. (1981) *Biochemistry 20*, 2141–2150.

Gorenstein, D. G., Luxon, B. A., Goldfield, E. M., Lai, K., & Vegeais, D. (1982) *Biochemistry 21*, 580–589.

Grosjean, H., Soll, D. G., & Crothers, D. M. (1976) *J. Mol. Biol. 103*, 499–519.

Gueron, M. (1971) *FEBS Lett. 19*, 264–266.

Gueron, M., & Shulman, R. G. (1975) *Proc. Natl. Acad. Sci. U.S.A. 72*, 3482–3485.

Jack, A., Ladner, J. E., & Klug, A. (1976) *J. Mol. Biol. 108*, 619.

Johnston, P. D., & Redfield, A. G. (1981) *Biochemistry 20*, 3996–4006.

Kan, L. S., Ts'o, P. O. P., Sprinzl, M., Haar, F. v. d., & Cramer, F. (1977) *Biochemistry 16*, 3143–3154.

Kayne, M. S., & Cohn, M. (1972) *Biochem. Biophys. Res. Commun. 46*, 1285–1291.

Kearns, D. R. (1976) *Prog. Nucleic Acid Res. Mol. Biol. 18*, 91.

Kim, S.-H. (1979) *Transfer RNA: Structure, Properties, and Recognition* (Schimmel, P. R., Soll, P., & Abelson, J. R., Eds.) p 115, Cold Spring Harbor Laboratories, Cold Spring Harbor, NY.

Kim, S.-H., Suddath, F. L., Quigley, G. J., McPherson, A., Sussman, J. L., Wang, A. H. J., Seeman, N. C., & Rich, A. (1974) *Science (Washington, D.C.) 185*, 435.

Labuda, D., & Porschke, D. (1980) *Biochemistry 19*, 3799–3805.

Labuda, D., & Porschke, D. (1982) *Biochemistry 21*, 49–53.

Lake, J. A. (1977) *Proc. Natl. Acad. Sci. U.S.A. 74*, 1903–1907.

Moller, A., Schwarz, U., Lipecky, R., & Gassen, H. G. (1978) *FEBS Lett. 89*, 263–266.

Moras, D., Comarmond, M. B., Fischer, J., Weiss, R., & Thierry, J. C. (1980) *Nature (London) 288*, 669–674.

Müller, A., Gueron, M., & Leroy, J. L. (1980) EMBO-FEBS tRNA Workshop, Strasbourg, France, July 16–21.

Patel, D. J. (1976) *Biopolymers 15*, 533–558.

Quigley, G. J., Wang, A. H. J., Seeman, N. C., Suddath, F. C., Rich, A., Sussman, J. L., & Kim, S. H. (1975) *Proc. Natl. Acad. Sci. U.S.A. 72*, 4866.

Quigley, G. J., Teeter, M. M., & Rich, A. (1978) *Proc. Natl. Acad. Sci. U.S.A. 75*, 64–68.

Reid, B. R., & Hurd, R. E. (1979) *Transfer RNA: Structure, Properties, and Recognition* (Schimmel, P. R., Soll, D., & Abelson, J. N., Eds.) p 177, Cold Spring Harbor Laboratories, Cold Spring Harbor, NY.

Robertson, J. M., Kahan, M., Wintermeyer, W., & Zachau, H. G. (1977) *Eur. J. Biochem. 72*, 117–125.

Salemink, P. J. M., Swarthof, T., & Hilbers, C. W. (1979) *Biochemistry 18*, 3477–3485.

Salemink, P. J. M., Reijerse, E. J., Mollevanger, L., & Hilbers, C. W. (1981) *Eur. J. Biochem. 115*, 635–641.

Schevitz, R. W., Podjarny, A. D., Krishnamachari, N., Hughes, J. J., & Sigler, P. B. (1979) *Transfer RNA:*

Structure, Properties, and Recognition (Schimmel, P. R., Soll, D., & Abelson, J. N., Eds.) p 133, Cold Spring Harbor Laboratories, Cold Spring Harbor, NY.
Schreier, A. A., & Schimmel, P. R. (1975) *J. Mol. Biol. 93*, 323–329.
Schwarz, U., Luhrmann, R., & Gassen, H. G. (1974) *Biochem. Biophys. Res. Commun. 56*, 807–814.
Sprinzl, M., Kramer, E., & Stehlik, D. (1974) *Eur. J. Biochem. 49*, 595.
Stout, C. D., Mizuno, H., Rao, S. T., Swaminathan, P., Rubin, J., Brennan, T., & Sundaralingam, M. (1978) *Acta Crystallogr., Sect. B 34*, 1529.
Sussman, J. L., Holbrook, S. R., Warrant, R. W., Church, G. M., & Kim, S. H. (1978) *J. Mol. Biol. 123*, 607.
Tabor, C. W., & Tabor, H. (1976) *Annu. Rev. Biochem. 45*, 285–306.
Takeda, Y., & Ohnishi, T. (1975) *Biochem. Biophys. Res. Commun. 63*, 611–617.
Urbanke, C., & Maass, G. (1978) *Nucleic Acids Res. 5*, 1551–1560.
Wagner, R., & Garrett, R. A. (1978) *FEBS Lett. 85*, 291–294.
Weiner, L. M., Backer, J. M., & Rezvukhin, A. I. (1974) *FEBS Lett. 41*, 40.
Woese, C. (1970) *Nature (London) 226*, 817–820.
Woo, N. H., Roe, B. A., & Rich, A. (1980) *Nature (London) 286*, 346–351.
Wright, H. T., Manor, P. C., Beurling, K., Karpel, R. L., & Fresco, J. R. (1979) *Transfer RNA: Structure, Properties, and Recognition* (Schimmel, P. R., Soll, D., & Abelson, I. N., Eds.) p 145, Cold Spring Harbor Laboratories, Cold Spring Harbor, NY.

Function of Transcription Termination Factor ρ in a Model Transcription System Using Synthetic Deoxyribonucleic Acid as Template†

Katsuya Shigesada* and Mutsuo Imai

ABSTRACT: The function of a transcription termination factor, ρ, has been studied by using several synthetic DNAs with simple repetitive base sequences as templates for transcription. ρ actually exhibits various effects on transcription depending on the base sequence of the template: (1) ρ terminates poly(A) synthesis with poly(dA)·poly(dT), poly(dT), or oligo(dT), leading to release of RNA from RNA polymerase. ρ also inhibits the synthesis of other homoribopolymers such as poly(U) directed by poly(dA)·poly(dT) and poly(C) and poly(I) directed by poly(dG)·poly(dC), presumably by a similar mechanism. (2) ρ inhibits the synthesis of another homoribopolymer, poly(G), directed by poly(dG)·poly(dC) at the step of initiation rather than propagation of transcription. (3) ρ stimulates rather than inhibits the synthesis of poly(A-C) and poly(G-U) directed by poly[d(A-C)]·poly[d(G-T)], presumably by enhancing the dissociation of transcription complexes. (4) ρ has no influence on the synthesis of poly(A-U) and poly(G-C) directed by poly[d(A-T)] and poly[d(G-C)], respectively. In the first case, but not otherwise, the effect of ρ is coupled with its RNA-dependent nucleosidetriphosphate phosphohydrolase activity, as is ρ-mediated transcription termination on natural templates. The implication of these results is discussed in reference to the current view that ρ acts on transcription complexes that have ceased elongation and causes release of RNA in an energy-requiring reaction.

The protein factor ρ from *Escherichia coli* causes termination of RNA synthesis at specific sites on the DNA template, with eventual release of RNA from DNA and RNA polymerase (Roberts, 1969, 1976). ρ has also an RNA-dependent nucleosidetriphosphate hydrolase activity (ρ NTPase)[1] (Lowery-Goldhammer & Richardson, 1974), which is required for its termination function (Howard & de Crombrugghe, 1976; Galluppi et al., 1976). Accumulated evidence has indicated that RNA polymerase by itself can recognize a termination site, temporarily halting its propagation (pause) there prior to and independent of the action of ρ (Darlix & Horaist, 1975; Rosenberg et al., 1978). These findings have culminated in the current view that the primary function of ρ is to release RNA from paused transcription complexes through its interaction with nascent RNA by an energy-dependent mechanism (Roberts, 1976; Richardson & Conaway, 1980; Shigesada & Wu, 1980). However, the molecular bases for the ρ-catalyzed termination as well as for the pausing of RNA polymerase are still poorly understood. Recently, DNA and RNA sequences have been determined for a number of ρ-dependent termination sites. Some of them have in common a specific feature, dyad symmetry preceding the termination point, which has been implicated in the pausing of RNA polymerase (Rosenberg et al., 1978; Küpper et al., 1978). However, there also have been reported different types of terminators lacking this feature (Wu et al., 1981; Reisbig & Hearst, 1981). Thus, no general explanation can yet be offered about the exact nature of the signal for the pausing event. Moreover, despite the abundance of sequence data, no definite clue has been obtained regarding another important question of what region or structural feature of nascent RNA serves as the target for the action of ρ.

† From the Department of Biochemistry, Institute for Virus Research, Kyoto University, Sakyo-ku, Kyoto 606, Japan. *Received April 30, 1982.* This work has been supported by grants from the Ministry of Education, Science and Culture, Japan.

[1] Abbreviations: NTP, nucleoside 5′-triphosphate; NTPase, nucleosidetriphosphate phosphohydrolase; AMP-PNP, 5′-adenylyl imidodiphosphate; GMP-PNP, 5′-guanylyl imidodiphosphate; UMP-PCP, uridine 5′-(β,γ-methylenetriphosphate); $NaDodSO_4$, sodium dodecyl sulfate; Tris, tris(hydroxymethyl)aminomethane; EDTA, ethylenediaminetetraacetic acid.

0006-2960/82/0421-5849$01.25/0